Am J Cancer Res 2024;14(12):5987-5998
www.ajcr.us /ISSN:2156-6976/ajcr0161180

Original Article

Prediction of axillary lymph node metastasis in breast cancer using an ultrasonic feature- and clinical data-based model

He Jin, Yunhai Gao

Department of General Surgery, Liaoning University of Traditional Chinese Medicine Affiliated Hospital, Shenyang 110032, Liaoning, China

Received October 14, 2024; Accepted December 22, 2024; Epub December 25, 2024; Published December 30, 2024

Abstract: The involvement of axillary lymph nodes (ALNs) is a critical prognostic factor affecting patient management and outcomes in breast cancer (BC). This study aims to comprehensively analyze the clinical data of BC patients, evaluate ultrasonic signs of ALNs, and explore the implications of a prediction model for ALN metastasis (ALNM) in early-stage BC patients based on ultrasonic features and clinical data. This study retrospectively analyzed ultrasonic features and clinical data from 216 patients diagnosed with unilateral invasive BC. The dataset was divided into a training (n = 162) and a validation set (n = 54) in a 3:1 ratio. Patients were then assigned into metastasis and non-metastasis groups depending on ALNM determined by pathological findings. Univariate analysis of various indicators followed by multivariate Logistic regression analysis was performed on the training set. A prediction model for ALNM in BC was established using binary logistic regression analysis, with its prediction performance evaluated by receiver operating characteristic curves (ROC) and area under the curve (AUC), and its reproducibility verified by the validation set. The pathological findings identified 57 (35.2%) cases of ALNM among 162 BC patients in the training set. Risk factors for ALNM included poorly differentiated type, high Ki-67 expression, lymph node (LN) aspect ratio ≥2, LN cortical thickness ≥1/2 of lymphatic hilum diameter, and mixed or peripheral LN blood flow. Protective factors included mass location in the outer upper quadrant and LN size >1 cm. A prediction model was established based on risk factors, with the equation being Logit (P) = -4.881 - 1.285 * differentiation degree + 1.485 * Ki-67 - 1.090 * lump quadrant - 0.956 * lymph node size + 1.244 * lymph aspect ratio + 1.032 * LN cortical thickness + 1.454 * LN medullary disappearance + 1.266 * LN blood flow. ROC analysis of the model yielded an AUC of 0.866, with a sensitivity of 80.7% and a specificity of 80.0%. The prediction model was validated using the validation set, producing an AUC of 0.809. These results demonstrate that color Doppler ultrasound effectively evaluates ALN status in BC patients. The prediction model for ALNM in BC shows strong accuracy and has potential clinical application.

Keywords: Breast cancer, axillary lymph nodes, metastasis, ultrasound

Introduction

Breast cancer (BC) is characterized by high malignancy and poor prognosis. The involvement of axillary lymph nodes (ALNs) is a critical prognostic factor affecting patient management and outcomes [1]. ALNs represent the most common metastatic pathway for BC. Axillary lymph node dissection (ALND) is an accurate way to stage BC, while ALN biopsy serves as the clinical standard for determining the necessity for ALND in BC patients [2]. Ultrasound-guided fine-needle aspiration biopsy is widely applied to preoperatively understand the ALNs of BC patients due to its advantages of small trauma, direct access to cells at suspicious sites, and convenient operation [3]. However, its limitations, including limited cell sample size and difficulties in accessing deep LNs, may result in false negatives. Additionally, puncture biopsy, although minimally invasive, carries risks such as bleeding and infection at the puncture site [4, 5]. Efforts have been made to establish optimal diagnostic methods for evaluating ALN status before treatment, aiming to avoid overtreatment of ALN-negative

https://doi.org/10.62347/VTEW9920

BC patients. Resection of involved LNs is crucial for effective treatment, while the evaluation of uninvolved LNs is vital for accurate staging. In recent years, radiological assessment of ALNs has gained importance, offering critical information for disease staging, treatment planning, and follow-up [6].

Imaging modalities, such as ultrasound (US), computed tomography (CT), and magnetic resonance imaging (MRI), are increasingly employed as ancillary tools for invasive procedures [7-9]. US is a non-invasive, repeatable, and widely employed technique that detects metastatic LNs based on morphological and functional criteria, such as size, shape, cortical thickness, margins, microcalcifications, and vascularization patterns assessed with color Doppler technology [10]. Meanwhile, the arteries and veins with low blood flow that are not visible in the conventional US can be visualized using the color flow imaging technique, which substantially enhances the sensitivity of hemodynamic assessment and offers a high reference value for determining the nature of ALNs.

Previous studies have developed prediction models for ALN metastasis using imaging or tumor markers, including US [11]. However, comprehensive models that incorporate a wide range of patient factors remain scarce. Consequently, this study aims to explore the risk factors for ALNM by retrospectively analyzing complete clinical records and ultrasonic features of invasive BC patients, providing clinicians with a foundation for selecting appropriate surgical approaches in the axillary area.

Materials and methods

Study population

A retrospective analysis was conducted on the ultrasonic features and clinical data of female patients with unilateral BC admitted to Liaoning University of Traditional Chinese Medicine Affiliated Hospital between January 2021 and December 2023. Inclusion criteria: (1) Unilateral lesion, confirmed as invasive carcinoma of no special type or invasive lobular carcinoma through core needle biopsy and surgical pathological examination; (2) No preoperative adjuvant radiotherapy or chemotherapy; (3) Underwent ipsilateral ALND or sentinel LN biopsy; (4) No evidence of distant metastasis; (5) Complete clinical and pathological data available. Exclusion criteria: (1) Occult BC, history of breast prosthesis implantation, or diagnosis of BC recurrence or distant metastasis; (2) Comorbid heart, brain, lung, and other organ diseases; (3) Malignancies other than BC; (4) History of radiotherapy and chemotherapy before BC resection; (5) Previous axillary, abdominal, or thoracic surgeries before BC surgery; (6) History of hematopoietic or lymphatic system tumors or blood system diseases; (7) Incomplete or missing clinical and medical records. Based on these criteria, a total of 216 eligible cases were included in this study. Data from 162 patients were allocated to the training set (3:1 ratio) for constructing the prediction model, while data from the other 54 patients comprised the validation set to verify the model. The study was approved by the Ethics Committee of Liaoning University of Traditional Chinese Medicine Affiliated Hospital.

Data collection and methods

(1) General data. Clinical data were collected from the hospital's medical record, including age, menstrual status, ultrasonic features, clinical staging, differentiation degree, pathological type, molecular subtyping, and Ki-67 expression.

(2) Ultrasonography. All patients underwent examination using a color Doppler US instrument with a probe frequency of 7.5-13.0 MHz. Two experienced sonographers observed and recorded the ultrasonic features of the masses and ALNs. A comprehensive scan was performed, in the order from the outer upper quadrant to the inner upper quadrant. Observations included the edges and morphology of the mass. The measurements were taken for mass features (maximum diameter, location, quadrant, morphology, boundary, calcification, and blood flow) and ALN features (size, long and short diameters, aspect ratio, cortical thickness, medullary disappearance, boundary, and blood flow).

Outcome determination

(1) Molecular subtyping: Molecular subtyping was performed based on the expression of estrogen receptor (ER), progesterone receptor

Table 1. Basic characteristics of breast cancer patients

	Training set (n = 162)	Validation set (n = 54)	t/χ^2	P
Age (yrs)			0.920	0.631
≤44	49	16		
44-60	77	29		
≥60	36	9		
Menopause			0.750	0.386
Yes	89	26		
No	73	28		
Clinical staging			0.232	0.630
I	96	34		
II	66	20		
Differentiation degree			3.094	0.213
Poorly differentiated	41	11		
Moderately differentiated	81	23		
Well differentiated	40	20		
Pathological type			0.353	0.552
Invasive breast carcinoma of no special type	110	39		
Invasive lobular carcinoma	52	15		
Molecular subtyping			2.898	0.408
Luminal A	65	20		
Luminal B	31	16		
HER2 overexpression	51	13		
Triple-negative	15	5		
Carbohydrate antigen 153 (U/mL)	28.75±4.87	29.08±4.69	0.435	0.664
Ki-67 expression status			0.752	0.386
Low expression	77	22		
High expression	85	32		
Postoperative lymph node metastasis			0.061	0.805
With	57	18		
Without	105	36		

(PR), human epidermal growth factor receptor 2 (HER2), and Ki-67. ER and PR expression ≥1% was considered positive. HER2 was determined through immunohistochemistry, with 0 or (+) being negative, (+++) being positive, and (++) required fluorescence in situ hybridization (FISH) for further classification, with positivity based on the presence of gene amplification. For Ki-67 expression, positive stained cell count <14% was defined as low Ki-67 expression, and ≥14% was defined as high Ki-67 expression [12, 13].

(2) LN metastasis (LNM): Negative (without LNM) or positive (with LNM) was determined according to the postoperative pathological examination results of LNs.

Statistical methods

Data analysis was conducted using SPSS 25.0. Count data were presented as frequency and proportion and analyzed using the chi-square test. Quantitative data were described as mean ± standard deviation and analyzed using the t-test. Multivariate Logistic regression analysis was performed to identify independent risk factors for ALNM, which were then incorporated to construct a prediction model. Logistic regression equation: Logit (P) = $a + b_1x_1 + ... + b_nx_n$, where a is the constant term representing the natural logarithm of the odds ratio when all independent variables (x) are 0. The predictive ability of the model was evaluated by receiver operating characteristic curves (ROCs) and

Table 2. Univariate analysis of pathological characteristics affecting ALNM in the training set

	ALNM		t/χ^2	P
	Positive (n = 57)	Negative (n = 105)		
Age			2.359	0.308
≤44	18	31		
44-60	23	54		
≥60	16	20		
Menopause			0.311	0.577
Yes	33	56		
No	24	49		
Clinical staging			0.168	0.682
I	35	61		
II	22	44		
Differentiation degree			6.321	0.042
Poorly differentiated	21	20		
Moderately differentiated	25	56		
Well differentiated	11	29		
Pathological type			0.209	0.648
Invasive breast carcinoma of no special type	40	70		
Invasive lobular carcinoma	17	35		
Molecular subtyping			4.684	0.196
Luminal A	20	45		
Luminal B	11	20		
HER2 overexpression	17	34		
Triple-negative	9	6		
Glycochain antigen 153 (U/mL)	29.54±4.01	28.32±5.25	1.524	0.129
Ki-67 expression status			6.917	0.009
Low expression	23	65		
High expression	34	40		

ALN: Axillary lymph node; ALNM: Axillary lymph node metastasis.

areas under the curve (AUCs). Statistical significance was set at P<0.05 with a test level of α = 0.05 for all analyses.

Results

Basic characteristics of BC patients in training and validation sets

The baseline data of 216 eligible BC patients are summarized in **Table 1**. According to a ratio of 3:1, 162 patients were assigned to the training set, and 54 cases comprised the validation set. No significant differences were observed between the two groups in terms of general data (P>0.05).

Univariate analysis of pathological characteristics of patients in the training set

Among the 162 patients in the training set, 57 cases tested positive for ALNM, while 105 were negative based on the pathological findings. The comparison of pathological features revealed significant differences between the groups in differentiation degree and Ki-67 expression status (all P<0.05). However, no significant differences were found in age, menopause status, clinical staging, pathological type, molecular subtyping, or the expression of CA153 and Ki67 (all P>0.05; **Table 2**).

Univariate analysis of ultrasonic characteristics of primary lesions in the training set

A comparison of the ultrasonic features of primary lesions showed statistical differences between groups in terms of the maximum diameter, quadrant, and calcification of the mass (all P<0.05). No statistical significance was observed in mass location, morphology, boundary, and blood flow (all P>0.05; **Table 3**).

Table 3. Univariate analysis of primary lesion-associated ultrasonic characteristics affecting ALNM in the training set

	ALNM		X^2	P
	Positive (n = 57)	Negative (n = 105)		
Maximum mass diameter (cm)			5.084	0.024
≤2	22	60		
>2	35	45		
Mass location			0.101	0.750
Left	30	58		
Right	27	47		
Lump quadrant			5.533	0.019
Outer upper quadrant	21	59		
Other quadrants	36	46		
Mass morphology			0.020	0.887
Regular	24	43		
Irregular	33	62		
Mass boundary			0.277	0.599
Defined	22	45		
Ill-defined	35	60		
Calcification			4.397	0.036
With	38	52		
Without	19	53		
Mass blood flow			3.118	0.078
With	37	53		
Without	20	52		

ALN: Axillary lymph node; ALNM: Axillary lymph node metastasis.

Univariate analysis of ultrasonic characteristics of ALNs in the training set

Inter-group comparison of ultrasonic characteristics of ALNs revealed statistical differences in LN size, aspect ratio, cortical thickness, medullary disappearance, boundary, and blood flow (all P<0.05; **Table 4**).

Multivariate analysis of ALNM in BC patients

Multivariate logistic regression analysis was conducted with ALNM status (0 = without, 1 = with) as the dependent variable, and variables with P<0.05 from the univariate analysis as independent variables. Before the analysis, categorical data were assigned values. Multivariate Logistic regression analysis identified poorly differentiated tumor, high expression of Ki-67, LN aspect ratio ≥2, LN cortical thickness ≥1/2 of lymphatic hilum diameter, and mixed or peripheral type LN blood flow as risk factors for ALNM in BC patients, and mass location in the outer upper quadrant and lymph node size >1 cm as protective factors (**Table 5**).

ROC analysis of factors influencing ALNM in the training set

ROC curves for the influencing factors obtained by logistic regression were constructed. The AUCs of differentiation degree, Ki-67 expression status, lump quadrant, LN size, LN aspect ratio, LN cortical thickness, LN medullary disappearance, and LN blood flow were 0.598, 0.608, 0.403, 0.418, 0.660, 0.645, 0.637 and 0.639, respectively (**Figure 1** and **Table 6**).

In a representative case, a hypoechoic nodule measuring 30.2*13.7*23.5 mm was seen in the 8 o'clock-1 o'clock direction posterior to and around the left glandular papilla. The nodule exhibited irregular morphology, lobulated and foliated margins, and ductal extension. Another mass extending toward the ducts was seen in the 2 o'clock direction. Internal echogenicity of the mass was heterogeneous, with punctate strong echoes and abundant blood flow signals. A 17.8*13.5 mm enlarged lymph node was seen in the left axilla, with clear boundary, irregular morphology, uneven internal echogenicity, absence of portal structure, and irregular blood flow signal. Ultrasound diagnosis: left breast space-occupying lesion (BI-RADS category 4c); abnormal left axillary lymph node (suggestive of metastatic). Pathologic findings showed invasive ductal carcinoma with ductal carcinoma in situ in the left breast, and cancer metastasis in the lymph nodes (**Figure 2**).

Construction of a prediction model for ALNM

The prediction model was constructed according to the regression coefficients and constant terms in **Table 5**. The equation: Logit (P) = -4.881 - 1.285 * differentiation degree + 1.485 * Ki-67 - 1.090 * lump quadrant - 0.956 * lymph node size + 1.244 * lymph aspect ratio

Table 4. Univariate analysis of ALN-associated ultrasonic characteristics affecting ANLM in the training set

	ALNM		χ^2	P
	Positive (n = 57)	Negative (n = 105)		
Lymph node size (cm)			3.976	0.046
≤1	37	51		
>1	20	54		
Lymph node aspect ratio			8.909	0.003
<2	17	65		
≥2	40	40		
Lymph node cortical thickness			14.461	0.000
<1/2 of lymphatic hilum diameter	16	60		
≥1/2 of lymphatic hilum diameter	41	45		
Lymph node medullary disappearance			11.151	0.000
Disappeared	39	43		
Not disappeared	18	62		
Lymph node boundary			6.090	0.014
Defined	21	60		
Ill-defined	36	45		
Lymph node blood flow			11.441	0.000
Mixed or peripheral	37	39		
Portal, dispersed, or no flow	20	66		

ALN: Axillary lymph node; ALNM: Axillary lymph node metastasis.

+ 1.032 * LN cortical thickness + 1.454 * LN medullary disappearance + 1.266 * LN blood flow. Using the predicted probability value as the test variable and the occurrence of ALN transition as the state variable, the model's discrimination ability was evaluated through ROC curve. The AUC was 0.866 (95% CI: 0.810-0.922), with a sensitivity of 80.7% and a specificity of 80.0%. The calibration curve indicated that the model demonstrated good accuracy and predictive ability (**Figure 3**).

Internal validation of the prediction model for ALNM in BC

To validate the prediction model, 54 BC patients from the validation set (18 with ALNM vs 36 without) were analyzed. The ultrasonic characteristics of the primary lesions and axillary lymph nodes in validation set are shown in **Table 7**. The model was verified using the validation set, achieving an AUC of 0.809 (95% CI: 0.671-0.947). The calibration curve further confirmed the model's good predictive ability for ALNM in BC patients (**Figure 4**).

Discussion

Research has revealed that the onset and progression of BC are the result of the synergistic effects of multiple genes and factors [14]. Axillary lymph node metastasis (ALNM) is crucial for BC staging. However, negative results from axillary lymph node dissection (ALND) in some early-stage BC patients highlight the need for a predictive model to assess ALNM risk. Such a model could help identify patients suitable for ALN surgery or ALND, thereby reducing the trauma and complications caused by unnecessary LN biopsy or ALND [15]. Furthermore, over-treatment of ALN-negative patients does not enhance local control or long-term survival outcomes [16]. Therefore, clarifying the characteristics of ALNM and investigating its related risk factors have positive significance for guiding clinical decision-making. This includes selecting reasonable surgical methods, formulating personalized treatment plans, and improving the accuracy of patient prognosis predictions.

This study revealed that the ALNM rate among BC patients was 34.7% (75/216). Regarding the characteristics of the primary tumor mass, univariate analysis indicated significant differences between patients with and without ALNM in terms of the maximum diameter, quadrant, and calcification of the mass in the training set. Larger primary tumors and greater tumor burden were associated with higher diffusion potential, a finding supported by previous studies [17, 18]. In fact, breast tumors are prone to occur in the outer upper quadrant [19], as reflected in the non-metastatic cases in this study. Legha et al. [20] reported that 62% of cases involved the upper and outer quadrants of the breast, possibly due to the larger amount of breast tissue in this region. Although women

Table 5. Multivariate analysis of factors affecting ALNM in breast cancer patients

	Assignment	β	SE	Wald	P	HR	95% CI
Constant	-	-4.881	1.014	23.189	0.000	0.008	-
Differentiation degree	(0 = well differentiated, 1 = moderately differentiated, 2 = poorly differentiated)						-
Moderately differentiated		0.827	0.611	1.835	0.176	2.288	0.691-7.575
Poorly differentiated		1.285	0.649	3.921	0.048	3.614	1.013-12.894
Ki-67 expression status	(0 = low expression, 1 = high expression)	1.485	0.475	9.771	0.002	4.414	1.740-11.198
Maximum mass diameter	(0 = ≤2, 1 = >2)	0.776	0.482	2.588	0.108	2.173	0.844-5.592
Lump quadrant	(0 = other quadrants, 1 = outer upper quadrant)	-1.090	0.512	4.532	0.033	0.336	0.123-0.917
Calcification	(0 = without, 1 = with)	0.516	0.470	1.205	0.272	1.676	0.666-4.214
Lymph node size	(0 = ≤1, 1 = >1)	-0.956	0.464	4.248	0.039	0.384	0.155-0.954
Lymph node aspect ratio	(0 = <2, 1 = ≥2)	1.244	0.474	6.902	0.009	3.470	1.372-8.777
Lymph node cortical thickness	(0 = <1/2 of lymphatic hilum diameter, 1 = ≥1/2 of lymphatic hilum diameter)	1.032	0.477	4.688	0.030	2.808	1.103-17.148
Lymph node medullary disappearance	(0 = not disappeared, 1 = disappeared)	1.454	0.472	9.481	0.002	4.278	1.696-10.792
Lymph node boundary	(0 = defined, 1 = ill-defined)	0.540	0.445	1.477	0.224	1.717	0.718-4.104
Lymph node blood flow	(0 = portal, dispersed, or no flow, 1 = mixed, or peripheral)	1.266	0.464	7.453	0.006	3.545	1.429-8.794

ALNM: Axillary lymph node metastasis.

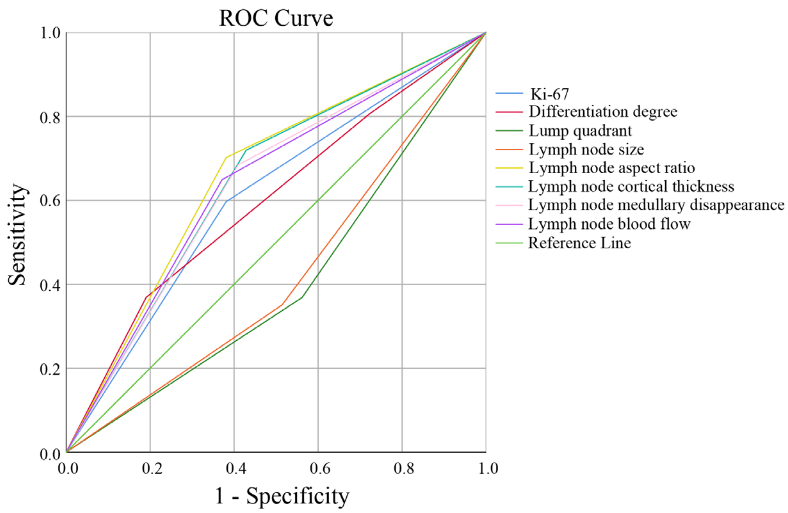

Figure 1. ROC curves for each index in predicting ALNM in BC patients. ROC: Receiver operating characteristic curves; ALNM: Axillary lymph node metastasis; BC: Breast cancer.

Table 6. ROC analysis of significant factors in predicting ALNM

	AUC	SE	P	95% CI
Differentiation degree	0.598	0.047	0.040	0.505-0.691
Ki-67 expression status	0.608	0.047	0.024	0.516-0.699
Lump quadrant	0.403	0.047	0.042	0.312-0.494
Lymph node size	0.418	0.047	0.086	0.327-0.510
Lymph node aspect ratio	0.660	0.045	0.001	0.573-0.748
Lymph node cortical thickness	0.645	0.045	0.002	0.557-0.733
Lymph node medullary disappearance	0.637	0.045	0.004	0.548-0.726
Lymph node blood flow	0.639	0.046	0.004	0.549-0.728

ROC: Receiver operating characteristic curves; ALNM: Axillary lymph node metastasis.

with tumors in the outer upper quadrant may have more LNs and a worse prognosis [21], they often receive more complete surgical treatment for tumor burden. In contrast, tumors in the inner quadrant are associated with a higher likelihood of undetected regional metastasis, making the outer upper quadrant a relative protective factor. Calcification, a major indicator of malignancy, results from calcium deposition in necrotic tumor cells. Evidence suggests a positive connection between tumor malignancy and the extent of calcification. Lu et al. [22] identified microcalcification as an independent predictor of lymph node metastasis (OR = 2.522, P = 0.003). Regarding the ultrasonic features of LNs, univariate analysis revealed significant differences in LN size, aspect ratio, cortical thickness, medullary disappearance, boundary, and blood flow between ALNM-positive and negative patients. Multivariate logistic regression analysis identified poorly differentiated tumor, high Ki-67 expression, LN aspect ratio ≥2, LN cortex thickness ≥1/2 of lymphatic hilum diameter, and mixed or peripheral LN blood flow as risk factors for ALNM. It is well known that breast cancer metastasis is related to the degree of pathological malignancy. Poorly differentiated tumors exhibit higher malignancy, stronger invasive potential, and greater likelihood of spreading to adjacent tissues, capillaries, and lymphatic vessels [23]. Ki-67, a key marker of tumor cell proliferation, distant metastasis and prognosis, has been linked to ALNM and other prognostic factors in BC [24, 25]. Interestingly, larger LN size (>1 cm) was found to be a protective factor, potentially due to inflammatory enlargement [26]. This finding underscores the need to consider LN size alongside the aspect ratio for accurate assessment. Healthy ALNs are typically oval-shaped, but metastasis induces significant changes, including increased volume, cortical thickening, and rounding, with notable alterations in the short diameter and cortical thickness [27, 28]. Cortical thickness is a widely studied parameter for predicting ALNM, although consensus on the optimal cut-off value remains elusive. Mainiero et al. [29] found that ALNs with a cortical thickness of ≥3 mm had a sensitivity of 94% and a specificity of 72% in predicting ALN positivity, while Cho et al. [30] reported a lower threshold of cortical thickness ≥2.5 mm with 85% sensitivity and 78% specificity. However, predicting ALN involvement solely based on ultrasonic features is still one-sided, as inflammation and reactive hyperplasia can mimic metastatic changes. Hence, it is necessary to

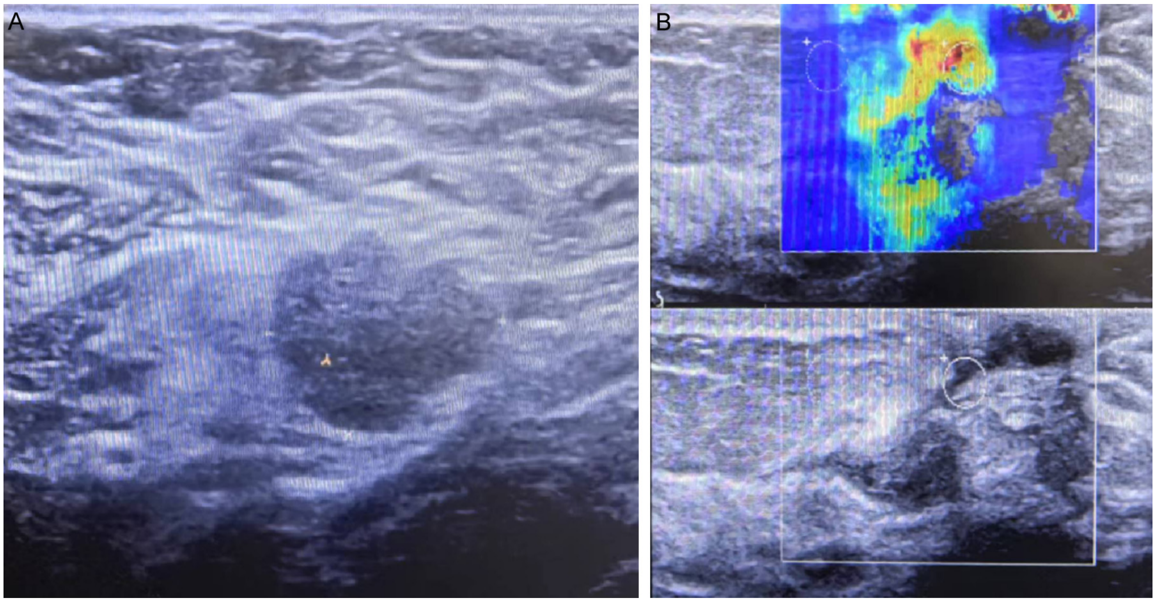

Figure 2. Ultrasound images of the mass and axillary lymph nodes of a typical case. A: Ultrasound images of the mass; B: Ultrasound images of the axillary lymph nodes.

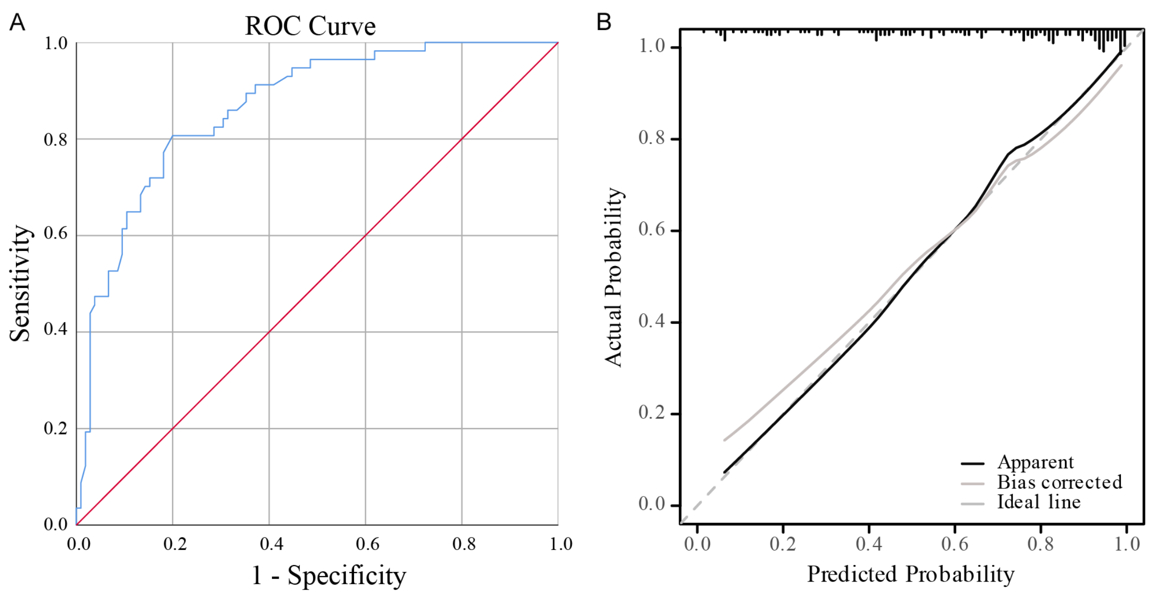

Figure 3. Prediction model for ALNM in BC patients. A: ROC curve of the prediction model for ALNM in BC patients in the training set; B: Calibration curve of the prediction model for ALNM in BC patients in the training set. ALNM: Axillary lymph node metastasis; ROC: Receiver operating characteristic curves; BC: Breast cancer.

combine clinical indicators with ultrasound findings to improve predictive efficiency. At the same time, medullary disappearance is also a risk factor. Metastatic invasion disrupts the LN capsule, cortex, and medulla, causing deformation and eccentricity of the medulla or nodal center [10]. The prediction model developed in this study, based on independent predictors, demonstrated good prediction value in both training and validation sets. The model combined multiple significant risk factors, providing complementary information that enhanced diagnostic efficiency, with certain guiding value for evaluating ALN status in BC patients.

Table 7. The ultrasonic characteristics of primary lesions and ALN in validation set

	Validation set (n = 54)
Maximum mass diameter (cm)	
≤2	27
>2	27
Mass location	
Left	24
Right	30
Lump quadrant	
Outer upper quadrant	29
Other quadrants	25
Mass morphology	
Regular	20
Irregular	34
Mass boundary	
Defined	21
Ill-defined	33
Calcification	
With	26
Without	28
Mass blood flow	
With	25
Without	29
Lymph node size (cm)	
≤1	33
>1	21
Lymph node aspect ratio	
<2	30
≥2	24
Lymph node cortical thickness	
<1/2 of lymphatic hilum diameter	23
≥1/2 of lymphatic hilum diameter	31
Lymph node medullary disappearance	
Disappeared	24
Not disappeared	30
Lymph node boundary	
Defined	32
Ill-defined	22
Lymph node blood flow	
Mixed or peripheral	24
Portal, dispersed, or no flow	30

ALN: Axillary lymph node.

Clinicians are encouraged to adopt a comprehensive approach by combining various indicators to enhance the evaluation of ALNs in BC patients.

Although the ALNM prediction model can accurately assess whether the ALN of breast cancer patients have metastasized, demonstrating certain clinical application value, this study still has some limitations. The indicators in this study were derived from a single-center database and retrospective analyses, with a relatively small sample size. Future research should validate the model with larger, multicenter datasets and focus on refining the quantitative indicators included in the model.

In conclusion, color Doppler ultrasound is a valuable tool for evaluating the ALN status of BC patients. The ALNM prediction model is effective in accurately assessing ALNM in BC patients and holds significant potential for clinical application.

Disclosure of conflict of interest

None.

Address correspondence to: Yunhai Gao, Department of General Surgery, Liaoning University of Traditional Chinese Medicine Affiliated Hospital, Shenyang 110032, Liaoning, China. Tel: +86-024-31961603; E-mail: H_60755@163.com

References

[1] Chang JM, Leung JWT, Moy L, Ha SM and Moon WK. Axillary nodal evaluation in breast cancer: state of the art. Radiology 2020; 295: 500-515.

[2] Gentilini OD, Botteri E, Sangalli C, Galimberti V, Porpiglia M, Agresti R, Luini A, Viale G, Cassano E, Peradze N, Toesca A, Massari G, Sacchini V, Munzone E, Leonardi MC, Cattadori F, Di Micco R, Esposito E, Sgarella A, Cattaneo S, Busani M, Dessena M, Bianchi A, Cretella E, Ripoll Orts F, Mueller M, Tinterri C, Chahuan Manzur BJ, Benedetto C and Veronesi P; SOUND Trial Group. Sentinel lymph node biopsy vs no axillary surgery in patients with small breast cancer and negative results on ultrasonography of axillary lymph nodes: the SOUND randomized clinical trial. JAMA Oncol 2023; 9: 1557-1564.

[3] Zheng H, Zhao R, Wang W, Liu X, Wang X, Wen C and Ren Y. The accuracy of ultrasound-guided fine-needle aspiration and core needle biopsy in diagnosing axillary lymph nodes in women with breast cancer: a systematic review and meta-analysis. Front Oncol 2023; 13: 1166035.

[4] Singh R, Deo SVS, Dhamija E, Mathur S and Thulkar S. To evaluate the accuracy of axillary

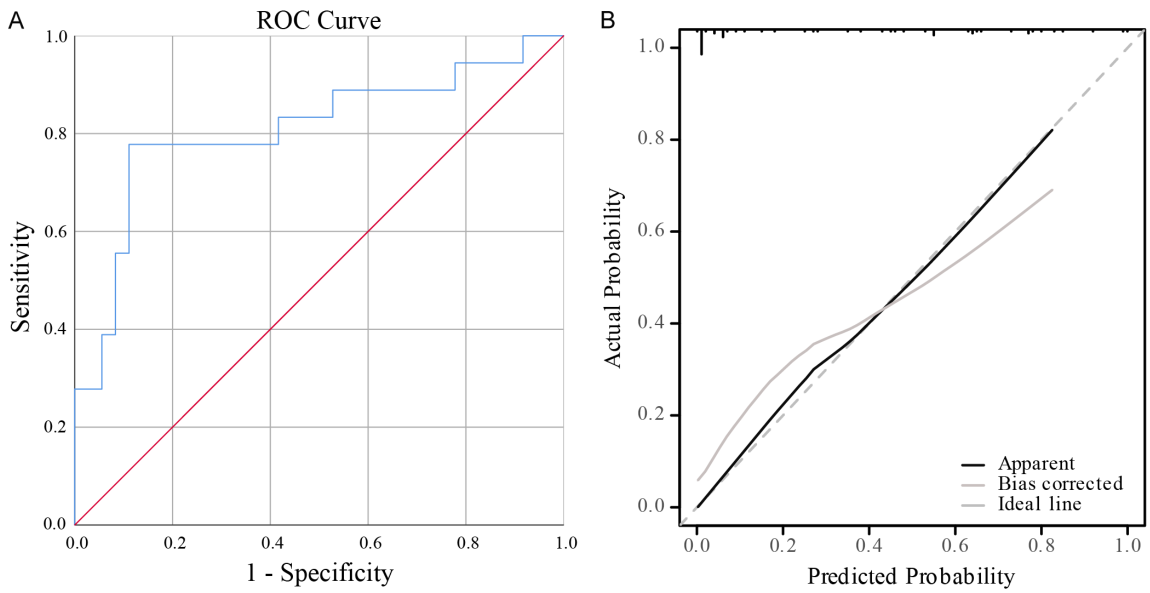

Figure 4. Internal validation of the prediction model for ALNM in BC patients. ALNM: Axillary lymph node metastasis; BC: breast cancer; ROC: Receiver operating characteristic curves.

staging using ultrasound and ultrasound-guided fine-needle aspiration cytology (USG-FNAC) in early breast cancer patients-a prospective study. Indian J Surg Oncol 2020; 11: 726-734.

[5] Winkler N, Buxton J, Freer P, Raps E, Barraza G, Boucher K, Riegert J and Factor R. Comparison of diagnostic sensitivity and procedure-related pain of concurrent ultrasound-guided fine-needle aspiration and core-needle biopsy of axillary lymph nodes in patients with suspected or known breast cancer. J Breast Imaging 2023; 5: 436-444.

[6] Marino MA, Avendano D, Zapata P, Riedl CC and Pinker K. Lymph node imaging in patients with primary breast cancer: concurrent diagnostic tools. Oncologist 2020; 25: e231-e242.

[7] Skarping I, Förnvik D, Zackrisson S, Borgquist S and Rydén L. Predicting pathological axillary lymph node status with ultrasound following neoadjuvant therapy for breast cancer. Breast Cancer Res Treat 2021; 189: 131-144.

[8] Zhang X, Liu Y, Luo H and Zhang J. PET/CT and MRI for identifying axillary lymph node metastases in breast cancer patients: systematic review and meta-analysis. J Magn Reson Imaging 2020; 52: 1840-1851.

[9] Davidson T, Shehade N, Nissan E, Sklair-Levy M, Ben-Haim S, Barshack I, Zippel D, Halevy A and Chikman B. PET/CT in breast cancer staging is useful for evaluation of axillary lymph node and distant metastases. Surg Oncol 2021; 38: 101567.

[10] Zhou J, Zhang B, Dong Y, Yu L, Gao T and Wang Z. Value on the diagnosis of axillary lymph node metastasis in breast cancer by color Doppler ultrasound combined with computed tomography. J BUON 2020; 25: 1784-1791.

[11] D'Angelo A, Orlandi A, Bufi E, Mercogliano S, Belli P and Manfredi R. Automated breast volume scanner (ABVS) compared to handheld ultrasound (HHUS) and contrast-enhanced magnetic resonance imaging (CE-MRI) in the early assessment of breast cancer during neoadjuvant chemotherapy: an emerging role to monitoring tumor response? Radiol Med 2021; 126: 517-526.

[12] Chlebowski RT, Col N, Winer EP, Collyar DE, Cummings SR, Vogel VG 3rd, Burstein HJ, Eisen A, Lipkus I and Pfister DG; American Society of Clinical Oncology Breast Cancer Technology Assessment Working Group. American Society of Clinical Oncology technology assessment of pharmacologic interventions for breast cancer risk reduction including tamoxifen, raloxifene, and aromatase inhibition. J Clin Oncol 2002; 20: 3328-3343.

[13] Yang C, Zhang J, Ding M, Xu K, Li L, Mao L and Zheng J. Ki67 targeted strategies for cancer therapy. Clin Transl Oncol 2018; 20: 570-575.

[14] Feng Y, Spezia M, Huang S, Yuan C, Zeng Z, Zhang L, Ji X, Liu W, Huang B, Luo W, Liu B, Lei Y, Du S, Vuppalapati A, Luu HH, Haydon RC, He TC and Ren G. Breast cancer development and progression: risk factors, cancer stem cells, signaling pathways, genomics, and molecular pathogenesis. Genes Dis 2018; 5: 77-106.

[15] Chen W, Wang C, Fu F, Yang B, Chen C and Sun Y. A model to predict the risk of lymph node

metastasis in breast cancer based on clinicopathological characteristics. Cancer Manag Res 2020; 12: 10439-10447.

[16] Hata C, Nakaoka H, Xiang Y, Wang D, Yang A, Liu D, Liu F, Zou Q, Wei L, Zheng K, Inoue I and You H. Germline mutations of multiple breast cancer-related genes are differentially associated with triple-negative breast cancers and prognostic factors. J Hum Genet 2020; 65: 577-587.

[17] Min SK, Lee SK, Woo J, Jung SM, Ryu JM, Yu J, Lee JE, Kim SW, Chae BJ and Nam SJ. Relation between tumor size and lymph node metastasis according to subtypes of breast cancer. J Breast Cancer 2021; 24: 75-84.

[18] Terada K, Kawashima H, Yoneda N, Toshima F, Hirata M, Kobayashi S and Gabata T. Predicting axillary lymph node metastasis in breast cancer using the similarity of quantitative dual-energy CT parameters between the primary lesion and axillary lymph node. Jpn J Radiol 2022; 40: 1272-1281.

[19] Chan S, Chen JH, Li S, Chang R, Yeh DC, Chang RF, Yeh LR, Kwong J and Su MY. Evaluation of the association between quantitative mammographic density and breast cancer occurred in different quadrants. BMC Cancer 2017; 17: 274.

[20] Legha M, Gandhi A, Gaur R, Bansal P and Chauhan S. Carcinoma breast: correlation study between tumor size, number of lymph nodes and metastasis. Int J Gen Can 2015; 2: 1-8.

[21] Siotos C, McColl M, Psoter K, Gilmore RC, Sebai ME, Broderick KP, Jacobs LK, Irwin S, Rosson GD and Habibi M. Tumor site and breast cancer prognosis. Clin Breast Cancer 2018; 18: e1045-e1052.

[22] Lu L, Xu C, Dai C, Xu X, Zhu L and Tan Y. Risk factors for axillary lymph node metastasis in breast cancer. Chin J Endocr Surg 2022; 16: 536-540.

[23] Arza IA, Khambri D, Rustam R, Novianti H and Yetti H. Relationship between molecular subtype, degree of differentiation, and lymph node metastasis with survival of breast cancer patients at Dr. M. Djamil General Hospital, Padang, Indonesia. Bioscientia Medicina: Journal of Biomedicine and Translational Research 2022; 6: 2779-2783.

[24] Al-Zawi A. Ki-67 proliferative index as a predictive tool for axillary pathological complete response in node-positive breast cancer. Int J Med Sci 2020; 7: 1-4.

[25] Bostanci ME, Mollaoglu MC and Karaday K. The relationship between Ki-67 index and axillary lymph node metastasis in breast carcinoma. Annals of Medical of Research 2020; 27: 1956.

[26] Danforth DN. The role of chronic inflammation in the development of breast cancer. Cancers (Basel) 2021; 13: 3918.

[27] Ramírez-Galván YA, Cardona-Huerta S, Elizondo-Riojas G, Álvarez-Villalobos NA, Campos-Coy MA and Ferrara-Chapa CM. Does axillary lymph node size predict better metastatic involvement than apparent diffusion coefficient (ADC) value in women with newly diagnosed breast cancer? Acta Radiol 2020; 61: 1494-1504.

[28] Pesapane F, Mariano L, Magnoni F, Rotili A, Pupo D, Nicosia L, Bozzini AC, Penco S, Latronico A, Pizzamiglio M, Corso G and Cassano E. Future directions in the assessment of axillary lymph nodes in patients with breast cancer. Medicina (Kaunas) 2023; 59: 1544.

[29] Mainiero MB, Cinelli CM, Koelliker SL, Graves TA and Chung MA. Axillary ultrasound and fine-needle aspiration in the preoperative evaluation of the breast cancer patient: an algorithm based on tumor size and lymph node appearance. AJR Am J Roentgenol 2010; 195: 1261-1267.

[30] Cho N, Moon WK, Han W, Park IA, Cho J and Noh DY. Preoperative sonographic classification of axillary lymph nodes in patients with breast cancer: node-to-node correlation with surgical histology and sentinel node biopsy results. AJR Am J Roentgenol 2009; 193: 1731-1737.